

Calculation of Potential Second Derivatives by Means of a Regularized Indirect Algorithm in the Boundary Element Method

H.B. Chen¹ and Masa. Tanaka²

Abstract: Highly accurate calculation of derivative values to the field variable is a key issue in numerical analysis of engineering problems. The boundary integral equations (BIEs) of potential second derivatives are of third order singularities and obviously the direct calculation of these high order singular integrals is rather cumbersome. The idea of the present paper is to use an indirect algorithm which is based on the regularized BIE formulations of the potential second derivatives, following the work of the present first author and his coworkers. The regularized formulations, numerical strategies and example tests are given for both potential first and second derivatives to make this work systematic and easier to observe the error sources. Numerical results show the validity of the newly proposed algorithm in the calculation of potential second derivatives at the boundary in two dimensional potential problems.

Keywords: boundary integral equation, potential second derivatives, regularized formulation, third order singularities, boundary element method

1 Introduction

Derivative calculation to the field variable is commonly met in numerical analysis of engineering problems. In elastic and elastoplastic problems, the displacement derivative is calculated for the construction of stress field. In potential problems, normal derivative at domain boundary is calculated for flux approximation. Especially in error estimation and the consequent adaptive mesh refinement, derivative values are used to calculate various norms of numerical errors in the finite element method (FEM) [Babuška and Yu (1987); Yu (1991a,b); Yazdani et al. (1997);

¹ CAS Key Laboratory of Mechanical Behavior and Design of Materials, Department of Modern Mechanics, University of Science and Technology of China, Hefei, Anhui 230026, China E-mail: hbchen@ustc.edu.cn

² Department of Mechanical Systems Engineering, Faculty of Engineering, Shinshu University, Nagano 380-8553, Japan

Moore (2004); Zienkiewicz (2006)] and the boundary element method (BEM) [Guiggiani (1996); Kita and Kamiya (2001); Chen et al. (2003); Martinez-Castro and Gallego (2005)]. Furthermore, sensitivity analysis also requires nodal values of the solution derivatives and the success or failure of such applications is to a great extent dependent on the accuracy of the extracted boundary solution derivatives [Guiggiani (1996); Zhang and Mukherjee (1991); Bonnet (1995); Bonnet and Guiggiani (1998); Ilinca and Pelletier (2007); Hou and Sheen (1993); Kita et al. (1999)]. In the context of BEM, derivative calculation generally induces increase of singularity in the boundary integrals and special regularization treatment should be applied. Specifically in BEM sensitivity analysis, material differentiation to singular BIEs [Kane et al. (1991); Bonnet (1997)] or regularized BIEs [Zhang and Mukherjee (1991); Bonnet (1995); Matsumoto et al. (1993)], up to second-order derivatives, does not increase the singularity order compared with their original ones. While nodal sensitivity analysis [Guiggiani (1996); Bonnet and Guiggiani (1998)] involves higher singularities which is the major concern of the present paper. In most cases, first derivatives to the field variable are considered and the relevant hypersingular integrals can be calculated by mean of reliable algorithms, see e.g. [Chen et al. (2003); Guiggiani et al. (1992); Sladek et al. (2003); Sladek and Sladek (1998); Chen et al. (1998); Chen et al. (2001); Chen et al. (2005a,b)]. Among them, a non-hyper-singular integral representation for displacement gradient was proposed by Okada et al. [Okada et al. (1988, 1989, 1990); Okada and Atluri (1994)], which is characterized by the integral variables being the boundary traction and displacement gradient. This algorithm was further developed to be performed through Petrov-Galerkin approaches and to acoustic problems by Han, et al. [Han and Atluri (2003, 2007); Atluri et al. (2003); Qian et al. (2004a,b); Han et al. (2005)].

However, there are still the requirements to evaluate the second derivatives to the field variable [Frangi and Guiggiani (2000); Guiggiani (1996)] and some attempts have been performed [Frangi and Guiggiani (2000); Karami and Derakhshan (1999); Chen (2004); Gallego and Martinez-Castro (2006); Gao (2006); Moore et al. (2007); Atluri (2005); Schwab and Wendland (1999)]. The boundary integral equations of potential second derivatives are of third order singularities; here the commonly met strong singularity is referred to as the first order singularity and the hypersingularity as the second order one. Obviously, such kind of high order singular integrals pose great challenges for numerical integration. Karami and Derakhshan (1999), Frangi and Guiggiani (2000) and Gallego and Martinez-Castro (2006) extended the direct approach, originally proposed for second order singular integrals by Guiggiani et al. (1992), to the third order singular ones. Gao (2006) proposed a new approach by simply removing the singular free terms, after expressing the

nonsingular parts of the kernels as polynomials of distance between source and field points, and using the Gauss quadrature for the remaining nonsingular integrals. Moore et al. (2007) calculated the second derivative values through ‘interior/exterior limit’ gradient algorithm in Galerkin BEM. The method of regularization of the BIEs for the first derivative has been shown to be easily extended to regularizing the BIEs for any order derivative of the primary variable by Atluri (2005). In computational mathematics, a successful bootstrapping algorithm for all derivatives was presented by Schwab and Wendland (1999), where (n+1)th order derivatives are computed from nth order by solving a succession of boundary integral problems. So far notable improvements have been achieved in these attempts, however the direct approach for second derivative calculation becomes more complicated; algorithm of Moore et al. encountered great difficulty for points at and near corners even for quadratic simple problem in a square domain; while Gao’s algorithm and the others need more tests of practical problems.

The present work is an extension of the regularized indirect algorithm for the calculation of potential or displacement first derivatives proposed by Chen et al. [Chen et al. (1998, 2001, 2005a,b, 2003, 2009); Jin and Chen (2004); Schnack and Chen (2001)] and its basic idea and primary numerical results had been reported orally by Chen (2004) in WCCM VI in conjunction with APCOM’04. The content of this paper is confined to two-dimensional (2D) Laplacian potential problem and the aim is to show how the potential second derivatives can be calculated by the proposed algorithm in an agreeable accuracy. The following part of this paper is organized as: first, the regularized formulation and numerical strategy for the calculation of potential first derivatives are presented; next come the corresponding parts of the potential second derivatives; following are four numerical tests to validate the present algorithms; at last come the discussions and conclusions.

2 Algorithm for potential first derivatives

2.1 Regularized Formulation

Consider a boundary value problem for a scalar variable $u(x)$ in classical potential field theory. Assuming no sources exist inside the considered domain Ω , the problem is governed by the Laplacian equation

$$\nabla^2 u(x) = 0 \text{ in } \Omega \tag{1}$$

and its boundary $\Gamma = \Gamma_u + \Gamma_p$ is subject to the mixed boundary conditions:

$$\left. \begin{aligned} u(x) &= \bar{u}(x) \quad x \in \Gamma_u \\ p(x) &= \frac{\partial u(x)}{\partial n(x)} = u_{,l}(x)n_l(x) = \bar{p}(x) \quad x \in \Gamma_p \end{aligned} \right\} \tag{2}$$

where the overbar denotes prescribed values on the boundary, $n_l(x)$ is the l -th Cartesian component of the outward normal at boundary point x ; $u_{,l}(x) = \frac{\partial u(x)}{\partial x_l}$, x_l is the Cartesian coordinate in l direction; $p(x)$ is the boundary flux. Here, $l = 1$ or 2 for 2D problem considered in this paper.

The potential integral equation for an internal point ξ is

$$u(\xi) = \int_{\Gamma} u^*(\xi, x) p(x) d\Gamma(x) - \int_{\Gamma} p^*(\xi, x) u(x) d\Gamma(x) \quad (3)$$

where $u^*(\xi, x)$ and $p^*(\xi, x)$ correspond to the usual free-space fundamental solutions, i.e.

$$u^*(\xi, x) = \frac{1}{2\pi} \ln\left(\frac{1}{r}\right) \quad , \quad p^*(\xi, x) = -\frac{r_{,l} n_l}{2\pi r} \quad (4)$$

and

$$r_i = r_i(\xi, x) = x_i(x) - x_i(\xi), \quad r = \sqrt{r_i r_i}, \quad r_{,i} = \frac{\partial r}{\partial x_i(x)} = \frac{r_i}{r}, \quad n_l = n_l(x) \quad (5)$$

x and ξ are the field and source points, respectively. Differentiating Eq. (3) with respect to $x_i(\xi)$ results in the integral representation of potential derivatives for internal point ξ as

$$u_{,i}(\xi) = \int_{\Gamma} u_{,i}^*(\xi, x) p(x) d\Gamma(x) - \int_{\Gamma} p_{,i}^*(\xi, x) u(x) d\Gamma(x) \quad (6)$$

where

$$\left. \begin{aligned} u_{,i}^*(\xi, x) &= \frac{\partial u^*(\xi, x)}{\partial x_i(\xi)} = \frac{r_{,i}}{2\pi r} \\ p_{,i}^*(\xi, x) &= \frac{\partial p^*(\xi, x)}{\partial x_i(\xi)} = \frac{n_i - 2 r_{,l} n_l r_{,i}}{2\pi r^2} \end{aligned} \right\} \quad (7)$$

As the source point ξ moves to the boundary, $u_{,i}^*(\xi, x)$ and $p_{,i}^*(\xi, x)$ show first order and second order singularities, respectively. To eliminate these singularities, a linear potential state is defined by the first two terms of the potential Taylor expansion at the source point ξ as

$$u^L(x) = u(\xi) + u_{,i}(\xi) r_i(\xi, x) \quad (8a)$$

The corresponding flux at the boundary is

$$p^L(x) = u_{,i}(\xi) n_i(x) \quad (8b)$$

In this state, the boundary integral equation of potential first derivative is

$$u_{,i}(\xi) = \int_{\Gamma} u_{,i}^*(\xi, x) p^L(x) d\Gamma(x) - \int_{\Gamma} p_{,i}^*(\xi, x) u^L(x) d\Gamma(x) \quad (9)$$

Subtracting Eq. (9) from Eq. (6), we get the regularized formulation of potential first derivative integral equation as

$$0 = \int_{\Gamma} u_{,i}^*(\xi, x) [p(x) - p^L(x)] d\Gamma(x) - \int_{\Gamma} p_{,i}^*(\xi, x) [u(x) - u^L(x)] d\Gamma(x) \quad (10)$$

Equation (10) is still valid (can be deduced in a similar way) for the source point ξ locating at the boundary, if the potential first derivatives at point ξ , i.e. $u_{,i}(\xi)$, exists at least in the Hölder sense. In this case,

$$\left. \begin{aligned} u(x) - u^L(x) &= 0[r(\xi, x)]^{1+\alpha} \\ p(x) - p^L(x) &= 0[r(\xi, x)]^{\alpha} \end{aligned} \right\} \quad 0 < \alpha \leq 1 \quad (11)$$

Thus Formulation (10) is at most weakly singular and it is the start point of the regularized indirect algorithm for the calculation of potential first derivatives. Telles and Prado (1993) presented a hyper-singular formulation for potential first derivatives in two dimensional problem, which has been shown equivalent to formulation (10) by Chen, et al. (2009).

2.2 Numerical Strategy

For 2D problem addressed in this paper, the matrix forms of $u^L(x)$ and $p^L(x)$ in Eq. (8) can be written as

$$u^L(x) = u(\xi) + [r_1(\xi, x) \ r_2(\xi, x)] \begin{Bmatrix} u_{,1}(\xi) \\ u_{,2}(\xi) \end{Bmatrix} = u(\xi) + \mathbf{R}_x^{\xi} \mathbf{U}'_{\xi} \quad (12a)$$

$$p^L(x) = [n_1(x) \ n_2(x)] \begin{Bmatrix} u_{,1}(\xi) \\ u_{,2}(\xi) \end{Bmatrix} = \mathbf{N}_x \mathbf{U}'_{\xi} \quad (12b)$$

For the regularized parts in Eq. (10), the standard interpolation scheme is given in terms of the nodal values and the element shape functions $N^{\alpha}(\eta)$ by

$$u(x) - u^L(x) = \sum_{\alpha} N^{\alpha}(\eta) [u_{\alpha} - u_{\alpha}^L] \quad (13a)$$

$$p(x) - p^L(x) = \sum_{\alpha} N^{\alpha}(\eta) [p_{\alpha} - p_{\alpha}^L] \quad (13b)$$

where u_{α} and p_{α} are the values of $u(x)$ and $p(x)$ at node α , respectively; $\eta = \eta(x)$ is the element local coordinate for the field point x . Thus, with $\xi = s$ and the

component $u_{,1}$ and $u_{,2}$ equations written together, the discretized form of Eq. (10) can be expressed as

$$\mathbf{0} = \sum_{k=1}^n \mathbf{G}'_{sk} [p_k - \mathbf{N}_k \mathbf{U}'_s] - \sum_{k=1}^n \mathbf{H}'_{sk} [u_k - u_s - \mathbf{R}_k^s \mathbf{U}'_s] \quad (14)$$

where n is the total number of discretization nodes, $\mathbf{G}'_{sk} = \begin{Bmatrix} G'_{sk1} \\ G'_{sk2} \end{Bmatrix}$, $\mathbf{H}'_{sk} = \begin{Bmatrix} H'_{sk1} \\ H'_{sk2} \end{Bmatrix}$, $G'_{ski} = \int_{-1}^1 u_{,i}^*(s, x(\eta)) N^k(\eta) J^k(x(\eta)) d\eta$, $H'_{ski} = \int_{-1}^1 p_{,i}^*(s, x(\eta)) N^k(\eta) J^k(x(\eta)) d\eta$, $N^k(\eta)$ is the shape function of node k at the calculating element, $J^k(x(\eta))$ is the related Jacobian function. In this paper, for non-simple problems only the mid-node of quadratic element is considered in order to retain enough continuity of the integrand during discretization, the same when calculating potential second derivatives.

Noting that $\mathbf{R}_s^s = \mathbf{0}$ and $p_s = \mathbf{N}_s \mathbf{U}'_s$, we have

$$\sum_{\substack{k=1 \\ k \neq s}}^n [\mathbf{G}'_{sk} \mathbf{N}_k - \mathbf{H}'_{sk} \mathbf{R}_k^s] \mathbf{U}'_s = \sum_{\substack{k=1 \\ k \neq s}}^n [\mathbf{G}'_{sk} p_k - \mathbf{H}'_{sk} (u_k - u_s)] \quad (15)$$

Equation (15) is the discretized formulation for the calculation of potential first derivatives at boundary nodes. Due to the at most weak singularity character for the integrals in Eq. (10), in the calculation of coefficients G'_{ski} and H'_{ski} ($k \neq s$) only Gaussian quadrature is required, thus this integration is as simple as doing a quadrature on a nonsingular integrand. Further comments on this algorithm will be given in Discussions. This algorithm has been reported in Chen et al. (2009) and used for calculating a reference solution for error estimation in Chen et al. (2005b). One can also refer to the corresponding algorithms in elasticity [Chen et al. (1998, 2001, 2003)].

3 Algorithm for potential second derivatives

3.1 Regularized Formulation

The potential second derivative integral equation can be given by differentiating Eq. (6) with respect to $x_j(\xi)$ as

$$u_{,ij}(\xi) = \int_{\Gamma} u_{,ij}^*(\xi, x) p(x) d\Gamma(x) - \int_{\Gamma} p_{,ij}^*(\xi, x) u(x) d\Gamma(x) \quad (16)$$

where

$$\left. \begin{aligned} u_{,ij}^*(\xi, x) &= \frac{\partial u_i^*(\xi, x)}{\partial x_j(\xi)} = \frac{2r_i r_j - \delta_{ij}}{2\pi r^2} \\ p_{,ij}^*(\xi, x) &= \frac{\partial p_i^*(\xi, x)}{\partial x_j(\xi)} = \frac{1}{\pi r^3} [r_i n_j + r_j n_i + r_l n_l (\delta_{ij} - 4r_{,i} r_{,j})] \end{aligned} \right\} \quad (17)$$

Similarly as the source point ξ moves from domain to the boundary, $u_{,ij}^*(\xi, x)$ and $p_{,ij}^*(\xi, x)$ show second order (hyper-) and third order singularities, respectively. To eliminate these singularities, a quadratic potential state is defined by the first three terms of the potential Taylor expansion at the source point ξ as

$$u^Q(x) = u(\xi) + u_{,i}(\xi)r_i(\xi, x) + \frac{1}{2}u_{,ij}(\xi)r_i(\xi, x)r_j(\xi, x) \quad (18a)$$

The corresponding flux at the boundary is

$$p^Q(x) = u_{,i}(\xi)n_i(x) + u_{,ij}(\xi)r_j(\xi, x)n_i(x) \quad (18b)$$

In this state, the boundary integral equation of potential second derivative is

$$u_{,ij}(\xi) = \int_{\Gamma} u_{,ij}^*(\xi, x)p^Q(x)d\Gamma(x) - \int_{\Gamma} p_{,ij}^*(\xi, x)u^Q(x)d\Gamma(x) \quad (19)$$

Subtracting Eq. (19) from Eq. (16), we get the regularized formulation of potential second derivative integral equation as

$$0 = \int_{\Gamma} u_{,ij}^*(\xi, x)[p(x) - p^Q(x)]d\Gamma(x) - \int_{\Gamma} p_{,ij}^*(\xi, x)[u(x) - u^Q(x)]d\Gamma(x) \quad (20)$$

The above formulation is still valid for the source point ξ locating at the boundary, if the potential second derivatives at point ξ , i.e. $u_{,ij}(\xi)$, exists at least in the Hölder sense. In this case,

$$\left. \begin{aligned} u(x) - u^Q(x) &= O[r(\xi, x)]^{2+\alpha} \\ p(x) - p^Q(x) &= O[r(\xi, x)]^{1+\alpha} \end{aligned} \right\}, \quad 0 < \alpha \leq 1 \quad (21)$$

Thus formulation (21) is at most weakly singular and it is the start point of the newly proposed Regularized Indirect Algorithm for the calculation of potential second derivatives.

3.2 Numerical Strategy

For 2D potential problem, noting that $u_{,12}(\xi) = u_{,21}(\xi)$ and $u_{,11}(\xi) = -u_{,22}(\xi)$, the matrix forms of the expressions in Eq. (18) can be written as

$$\begin{aligned} u^Q(x) &= u(\xi) + [r_1(\xi, x) \ r_2(\xi, x)] \begin{Bmatrix} u_{,1}(\xi) \\ u_{,2}(\xi) \end{Bmatrix} \\ &\quad + \frac{1}{2} \{r_1^2(\xi, x) - r_2^2(\xi, x)\} r_1(\xi, x) r_2(\xi, x) \begin{Bmatrix} u_{,11}(\xi) \\ u_{,12}(\xi) \end{Bmatrix} \\ &= u(\xi) + \mathbf{R}_x^\xi \mathbf{U}'_\xi + \bar{\mathbf{R}}_x^\xi \mathbf{U}''_\xi \end{aligned} \tag{22a}$$

$$\begin{aligned} p^Q(x) &= [n_1(x) \ n_2(x)] \begin{Bmatrix} u_{,1}(\xi) \\ u_{,2}(\xi) \end{Bmatrix} \\ &\quad + [n_1(x) r_1(\xi, x) - n_2(x) r_2(\xi, x) \ n_1(x) r_2(\xi, x) + n_2(x) r_1(\xi, x)] \begin{Bmatrix} u_{,11}(\xi) \\ u_{,12}(\xi) \end{Bmatrix} \\ &= \mathbf{N}_x \mathbf{U}'_\xi + \bar{\mathbf{N}}_x^\xi \mathbf{U}''_\xi \end{aligned} \tag{22b}$$

Similar to Expression (13), the regularized parts in Eq. (20) are interpolated by

$$\left. \begin{aligned} u(x) - u^Q(x) &= \sum_{\alpha} N^{\alpha}(\eta) [u_{\alpha} - u_{\alpha}^Q] \\ p(x) - p^Q(x) &= \sum_{\alpha} N^{\alpha}(\eta) [p_{\alpha} - p_{\alpha}^Q] \end{aligned} \right\} \tag{23}$$

Thus, with $\xi = s$ and the component $u_{,11}$ and $u_{,12}$ equations written together, the discretized form of Eq. (20) can be expressed as

$$\mathbf{0} = \sum_{k=1}^n \mathbf{G}_{sk}'' [p_k - \mathbf{N}_k \mathbf{U}'_s - \bar{\mathbf{N}}_k^s \mathbf{U}''_s] - \sum_{k=1}^n \mathbf{H}_{sk}'' [u_k - u_s - \mathbf{R}_k^s \mathbf{U}'_s - \bar{\mathbf{R}}_k^s \mathbf{U}''_s] \tag{24}$$

where $\mathbf{G}_{sk}'' = \begin{Bmatrix} G_{sk11}'' \\ G_{sk12}'' \end{Bmatrix}$, $\mathbf{H}_{sk}'' = \begin{Bmatrix} H_{sk11}'' \\ H_{sk12}'' \end{Bmatrix}$, $G_{skij}'' = \int_{-1}^1 u_{,ij}^*(s, x(\eta)) N^k(\eta) J^k(x(\eta)) d\eta$, $H_{skij}'' = \int_{-1}^1 p_{,ij}^*(s, x(\eta)) N^k(\eta) J^k(x(\eta)) d\eta$.

Noting that $\mathbf{R}_s^s = \bar{\mathbf{N}}_s^s = \bar{\mathbf{R}}_s^s = \mathbf{0}$ and $p_s = \mathbf{N}_s \mathbf{U}'_s$, we have

$$\sum_{\substack{k=1 \\ k \neq s}}^n [\mathbf{G}_{sk}'' \bar{\mathbf{N}}_{kk}^s - \mathbf{H}_{sk}'' \bar{\mathbf{R}}_k^s] \mathbf{U}''_s = \sum_{\substack{k=1 \\ k \neq s}}^n [\mathbf{G}_{sk}'' (p_k - \mathbf{N}_k \mathbf{U}'_s) - \mathbf{H}_{sk}'' (u_k - u_s - \mathbf{R}_k^s \mathbf{U}'_s)]$$

(25)

Equation (25) is the discretized formulation of present algorithm for the calculation of potential second derivatives at boundary nodes. Similar to the case in potential first derivative calculation, due to the at most weak singularity character, the calculation of G''_{skij} and H''_{skij} ($k \neq s$) only requires a Gaussian quadrature. When implementing this equation, the potential first derivative vector \mathbf{U}'_s should be given in advance, which can be calculated through the regularized algorithm presented in last section.

4 Numerical examples

In all examples, quadratic continuous isoparametric boundary element and 10 point Gaussian quadrature are employed. For 2D Laplacian potential problem, as mentioned above, $u_{,12}(\xi) = u_{,21}(\xi)$ and $u_{,11}(\xi) = -u_{,22}(\xi)$. Therefore, a relative error for the evaluated nodal potential second derivatives can be defined as $\varepsilon''_i = \frac{\sqrt{(\tilde{u}''_{,11} - u''_{,11})^2 + (\tilde{u}''_{,12} - u''_{,12})^2}}{\frac{1}{n} \sum_{k=1}^n \sqrt{(u''_{,11})^2 + (u''_{,12})^2}} \times 100\%$, where $\tilde{u}''_{,11}$ and $\tilde{u}''_{,12}$ are the calculated potential sec-

ond derivatives at node i ; $u''_{,11}$ and $u''_{,12}$ are the respective exact values; n is the total number of the calculated nodes. The corresponding nodal relative error for potential first derivatives is defined as $\varepsilon'_i = \frac{\sqrt{(\tilde{u}'_{,1} - u'_{,1})^2 + (\tilde{u}'_{,2} - u'_{,2})^2}}{\frac{1}{n} \sum_{k=1}^n \sqrt{(u'_{,1})^2 + (u'_{,2})^2}} \times 100\%$. The above

relative errors are in fact scaled local nodal errors. They are different from the conventional nodal relative error which is usually defined by the nodal error normalized by the local exact solution. The reason we adopt this new definition is that BEM solution has a global effect and for some local small values which might be around zero, a big conventional relative error might correspond to a very small local nodal error and it is of course meaningless, however present error definition can avoid this misleading.

Example 1: A square area of side length 8 is analyzed, as shown in Fig. 1. The potential distribution is $u = x_1^2 + 3x_1x_2 - x_2^2 + 4$ and the problem is defined as the potential at sides AD and BC and the flux at the other two sides are prescribed. This problem is analyzed with one quadratic element each side. The nodal potential second derivatives calculated by the present algorithm are almost the same with the exact solutions, i.e. six significant digits the same with the exact solutions, for all the eight nodes in this discretization. While the nodal potential first derivatives calculated are of seven significant digits the same with the exact solutions. Therefore, it can be concluded that the present indirect algorithm passes the numerical patch test.

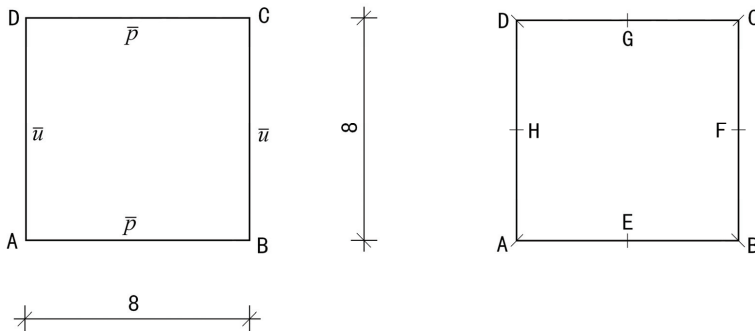


Figure 1: A square area and its discretization for analysis

Example 2: The warping function of an elliptical bar under torsion is analyzed, which is a Laplacian problem with exact solution $u = \frac{b^2 - a^2}{b^2 + a^2} x_1 x_2 + C$ and boundary condition $\frac{\partial u}{\partial n} = \frac{b^2 - a^2}{\sqrt{a^4 x_2^2 + b^4 x_1^2}} x_1 x_2$, where C is a constant and a and b are respectively the longer and shorter semidiameters of the elliptical area. The dimensions are assumed to be $a=10$, $b=5$ and $C=20$. By use of symmetry, one quarter of the elliptical section is analyzed. As shown in Fig. 2, the domain in the first quadrant of the elliptical section is considered for analysis, where the two sides along the coordinate axes are potential prescribed and the curve side flux prescribed.

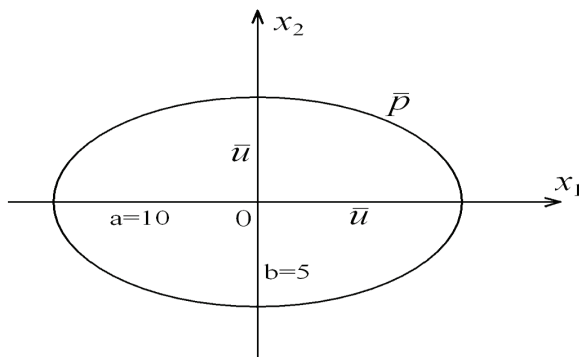


Figure 2: Geometrical definitions of an elliptical bar under torsion

Two meshes, as shown in Fig. 3, are considered for comparing the results. In order

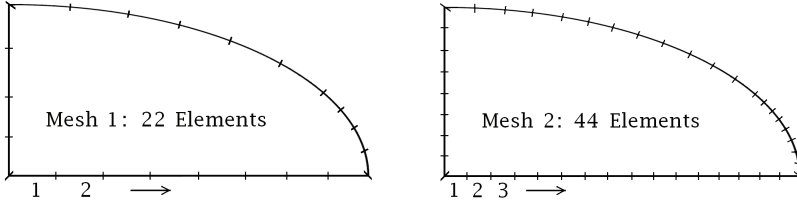


Figure 3: Mesh definition of the one quarter area

to satisfy the continuity condition of the regularized formulations, hereafter only the element mid-nodes are adopted in calculation. It can be seen from Fig. 4 that the nodal relative errors of potential first derivatives are in low level even in the coarser Mesh 1 and the errors reduce significantly and consistently when the mesh is subdivided to Mesh 2. The horizontal axes shows the Calculation Node numbers in Mesh 2 and the calculation nodes in Mesh 1 have been renumbered accordingly so as to plot them in one figure, the same treatment hereafter. For the calculation of potential second derivatives, from Fig. 5 we can see that relatively larger errors happen around the two corners in Mesh 1. In Mesh 2, the numerical results improve significantly and the maximum error is no more than 2.5%. These results show that both potential first and second derivatives can be well calculated by means of the present regularized indirect algorithms and the results are convergent as the mesh is subdivided.

Example 3: The third example consists of an L shaped domain shown in Fig. 6, with \bar{p} and \bar{u} taking values such that the analytical solution is $u = r^{\frac{2}{3}} \sin(\frac{2\theta}{3})$, where r and θ are the cylindrical co-ordinates with respect to the origin of the Cartesian axes. The prescribed boundary conditions and the symmetry axis of the problem are also shown in Fig. 6.

This problem was analyzed in the Cartesian co-ordinate system and two of its discretizations are shown in Fig.7, a further uniform subdivision from Mesh 2 to a 128 element discretization called Mesh 3 is also used for accuracy comparison. The exact solutions of this problem are $u_{,1} = \frac{2}{3}r^{-\frac{1}{3}} \sin(-\frac{\theta}{3})$, $u_{,2} = \frac{2}{3}r^{-\frac{1}{3}} \cos(-\frac{\theta}{3})$ and $u_{,11} = \frac{2}{9}r^{-\frac{4}{3}} \sin(\frac{4\theta}{3})$, $u_{,12} = -\frac{2}{9}r^{-\frac{4}{3}} \cos(\frac{4\theta}{3})$. It can be seen that, at the reentrant corner, weak and strong singularities happen for the potential first and second derivatives, respectively. Therefore, it is a problem with relatively strong variation of the field variables. Like some stress singularity problems in linear elasticity, most algorithms including the present one do not work at the singularity point, but work for nodes with a distance of a few elements to the reentrant corner.

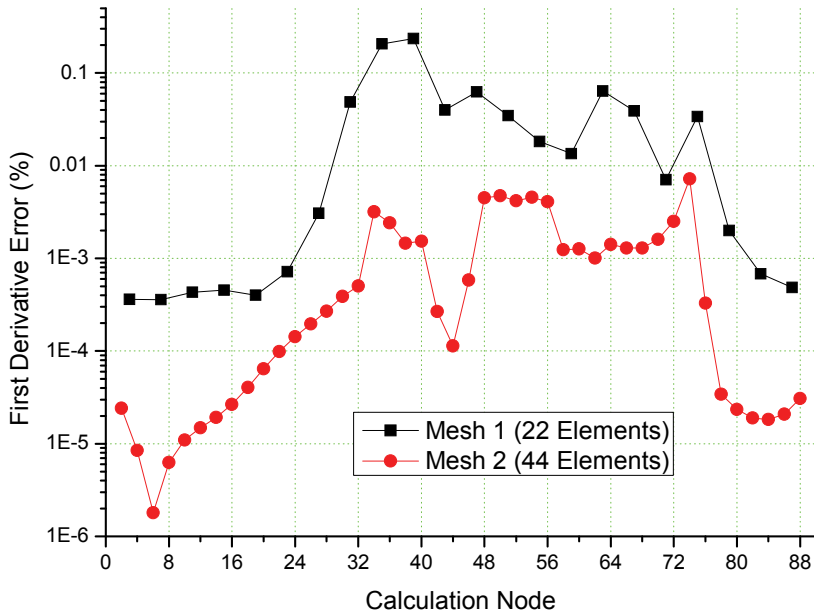


Figure 4: Relative error of potential first derivatives in Example 2

Due to symmetry, only half of the nodal errors are given. Fig. 8 shows that the numerical errors increase significantly as the calculation point closes to the reentrant corner from a certain distance. This is due to the strong variation of the potential first derivatives near the reentrant corner and larger interpolation errors thereby. Whereas the overall errors are in low level, i.e. lower than 0.7%, from the third element mid-nodes for all the three discretizations and the calculation errors reduce consistently as the mesh is subdivided. Fig. 9 presents the nodal errors of potential second derivatives for the three meshes; similar phenomena can be observed as in the first derivative calculation, except now with higher error levels. The higher errors in second derivative calculation are correspondent with the higher singularities in the kernel and the higher variation of physical value, furthermore the errors of first derivatives will be introduced in during this calculation.

Example 4: This example is of the same physical problem with Example 3, however with different boundary contour by consisting of a $3/4$ circular domain as shown in Fig. 10. The prescribed boundary conditions and the symmetry axis of the problem are also shown in Fig.10. This example is designed to compare with Example 3 for observing the influence of different boundary contour on the numer-

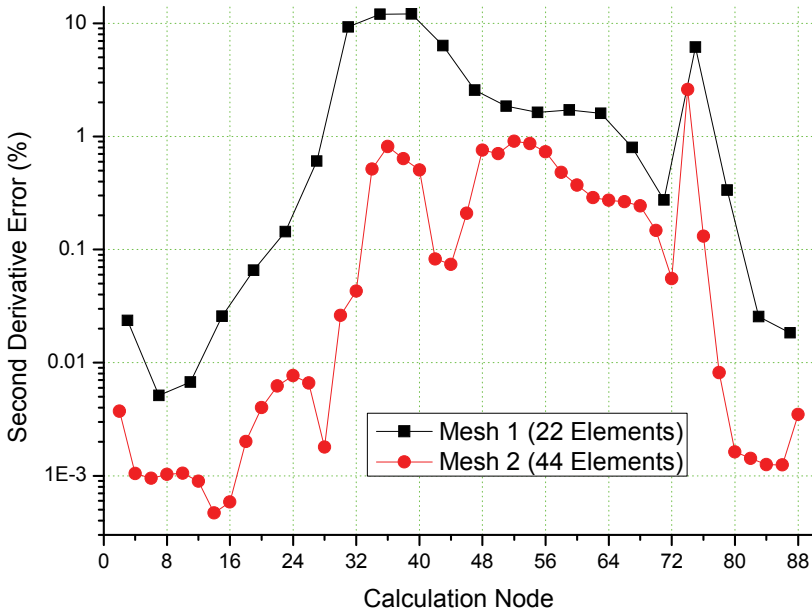


Figure 5: Relative error of potential second derivatives in Example 2

ical results. Example 3 consists of only straight boundaries, while this example composes of both straight and curve boundaries.

This problem was also analyzed in the Cartesian co-ordinate system and two of its discretizations are shown in Fig. 11, a further uniform subdivision from Mesh 2 to a 128 element discretization called Mesh 3 is also used for accuracy comparison. Figs. 12 and 13 show that errors near the reentrant corner are similar to those in Example 3 and, in the curve parts, the errors reduce consistently with respect to the distance between the calculation point and the convex corner. The consistent error reduction with respect to mesh subdivision and higher errors for second derivatives are the same as in Example 3. However, carefully comparing the respective figures in these two examples, we can find that the errors in Example 4 are smaller than those in Example 3 for both first and second derivative results. The reason of this phenomenon is that, for this physical problem and boundary contours, the interpolation error of the field variables has bigger influence than that of geometry.

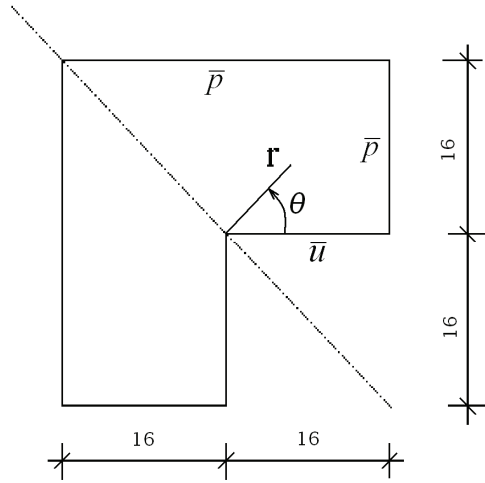


Figure 6: An L shape domain with reentrant corner singularity

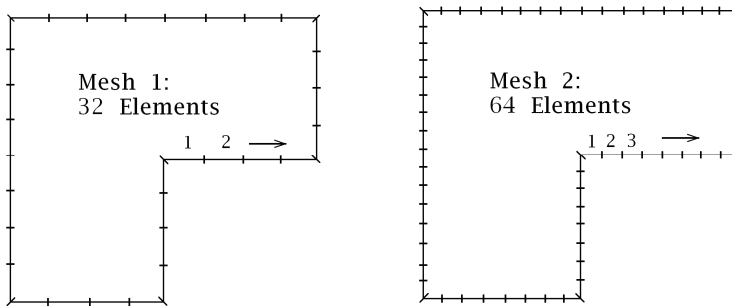


Figure 7: Two discretization schemes of the L shape domain

5 Discussions

5.1 On the treatment of singular integrals in the regularized indirect algorithm

The main feature of the regularized indirect algorithm presented in this paper is its simple implementation, where all numerical integrations are performed by Gaussian quadrature as done for non-singular integrals. The nodal coefficients of inaccurate integrations near the source point are manipulated and the errors reduce

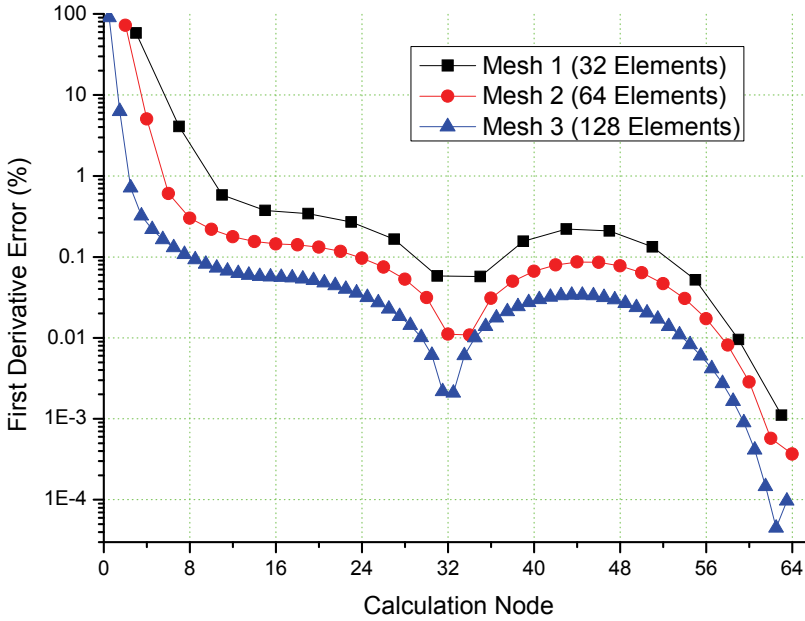


Figure 8: Relative error of potential first derivatives in Example 3

to an agreeable degree according to the relationship of the discretized form of the regularized formulations. For the isoparametric quadratic element used in this paper, during interpolation the continuity of integrand at element mid-node will retain to a degree to mathematically ensure the existence of all the singular integrals. If there are explicit expressions for the regularized parts in the integration space, the product of singular kernel and the regularized parts will become nonsingular and, of course, only Gaussian quadrature is needed in numerical integration. However, present case is that the regularized parts contain derivative unknowns and the integrand is the product of singular kernel and the interpolation shape function. Although Gaussian quadrature can not integrate precisely these highly singular integrands, the singularity elimination function of the regularized parts retains through the post treatments to the inaccurate coefficients, in which the utmost inaccurate coefficients related to the potential and flux at the singular point are eliminated. Furthermore, from the last calculating formulations (15) and (25), we can find that the non-eliminated inaccurate coefficients remain in the two sides of the formulations and they possess the same influence in each side. Therefore, the present indirect algorithm is much different from the direct ones by doing the regulariza-

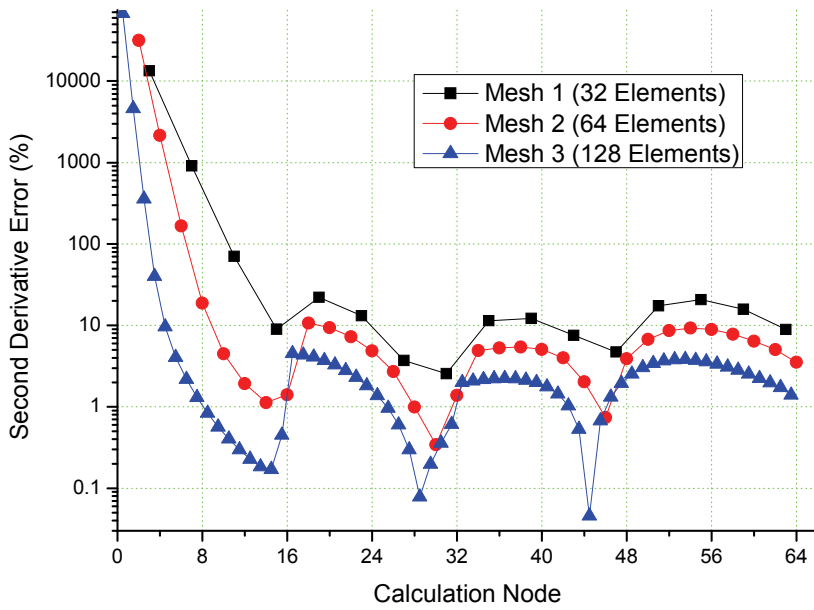


Figure 9: Relative error of potential second derivative in Example 3

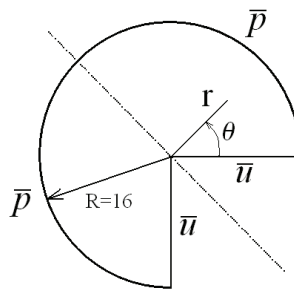


Figure 10: A 3/4 circular domain with reentrant corner singularity for derivative values

tion after integration.

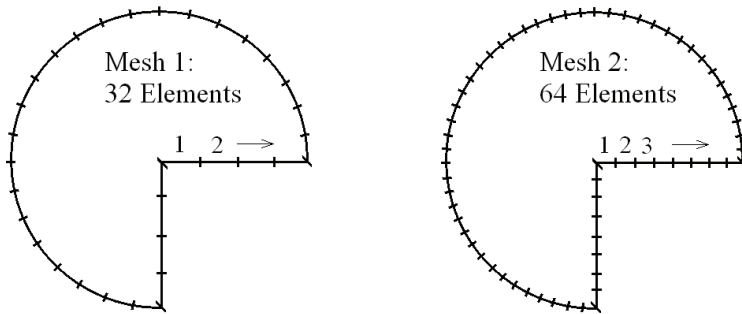


Figure 11: Two discretization schemes of the 3/4 circular domain

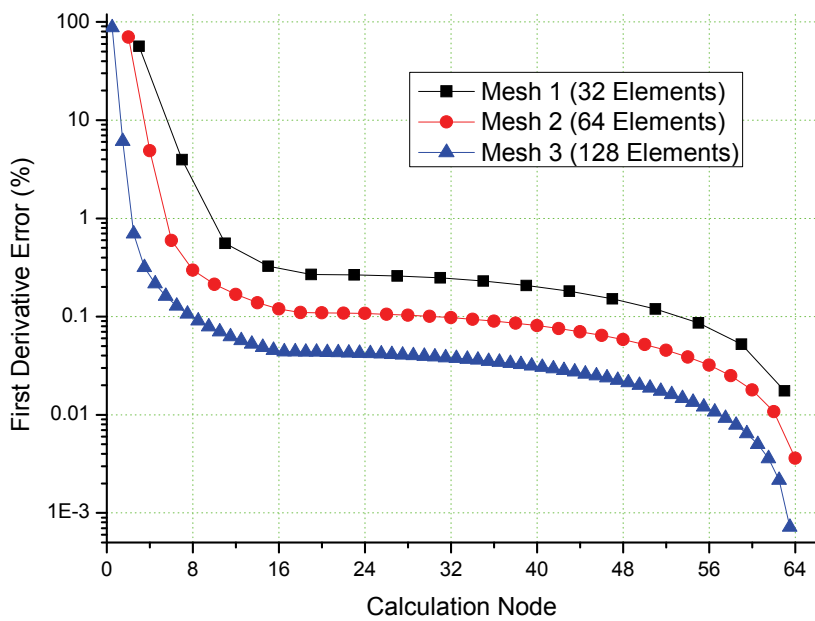


Figure 12: Relative error of potential first derivatives in Example 4

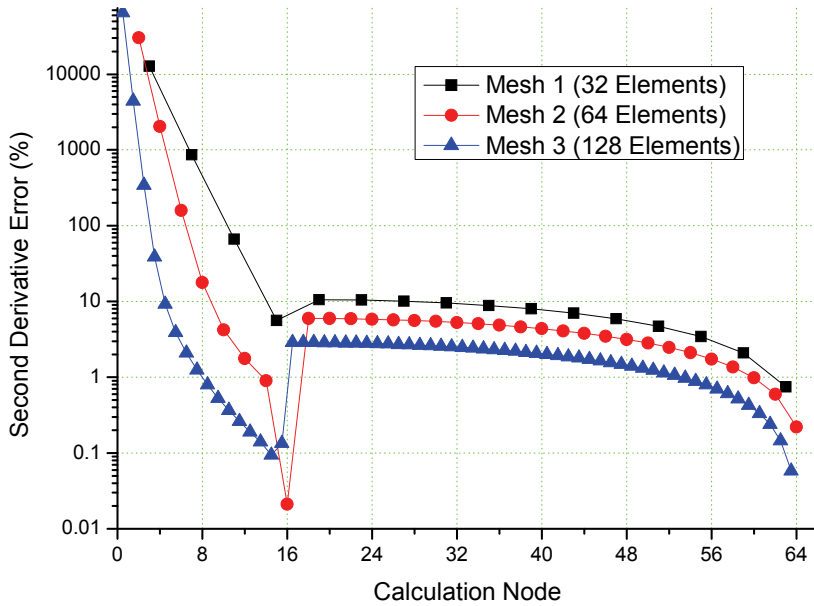


Figure 13: Relative error of potential second derivatives in Example 4

5.2 On the influence of interpolation errors

Compared with the calculation of first derivative values, the second derivative calculation is more sensitive to the interpolation error and the primary solution error. Example 1 is a simple problem with straight domain boundary and quadratic potential variation (constant second derivatives). No error occurs in the interpolation of boundary geometry and variables (potential and flux), and numerical test shows that the third order singularity in BIE formulation can be completely eliminated by the present algorithm. The second example is also with a quadratic potential variation, however one side of its boundary is elliptic. When applying the isoparametric quadratic element, interpolation error on this boundary is unavoidable. On the other hand, Example 3 has a simple domain boundary, however the field potential varies sharply near the reentrant corner and thus error is again unavoidable in the interpolation of boundary variables. In these two examples, potential second derivatives at element end nodes are basically incorrect even in the refined meshes, thus only the element mid-node results are presented. This shows that the interpolation error of boundary geometry or field variables is magnified to a much larger extent, compared with those in the calculation of potential first derivatives. A similar situation

was also found in the work of Martinez-Castro and Gallego (2005) and Gallego and Martinez-Castro (2006), where the tangential BIE residual are collocated only at the quadratic element mid-nodes. Therefore, for the element interpolation function higher continuity is required in the calculation of second derivative values.

Example 4 is designed to compare with Example 3 for careful observation of the influences of different kinds of interpolation errors. Example 4 is defined from Example 3 by replacing the outer straight boundaries, other than the two connected to the reentrant corner, with a $3/4$ circle line. There is no interpolation error in the approximation of boundary contour for Example 3, however there is for Example 4. Observing the numerical results, for points far away from the reentrant corner, both the first and second derivative errors for Example 4 are lower than those of Example 3, with more obvious for second derivative errors. Thus in this test the interpolation errors for physical values have bigger influence to the final results than those for boundary contours (co-ordinates). For these examples, it should be noted that non-uniform distribution of nodes, with more locating near the singularity point, is quite possible to further improved the numerical results.

5.3 On the validity of the present indirect algorithm

Here we discussed the validity of the present indirect algorithm for the calculation of potential first and second derivatives, especially in comparison with other parallel algorithms. For most commonly used isoparametric quadratic element, numerical tests in this paper have shown that the potential first derivatives at element mid-nodes can be calculated with excellent accuracy, it has also been shown that the results at element end-nodes are still of good accuracy compared with those obtained by the conventional treatment which differentiates the interpolation function [Schnack and Chen (2001); Chen et al. (2005b)]. The same situation has been observed in elastic BEM for the calculation of displacement first derivatives and boundary nodal stresses [Chen et al. (1998, 2001)], which were further used for error estimations [Chen et al. (2003)]. For the indirect algorithm for potential second derivatives, numerical tests in this paper have shown its correctness for quadratic element mid-nodes. The numerical accuracy should be further improved by adopting some careful treatments, e.g. using the singularity treatment proposed by Gao (2006), and the results at element end nodes might reach an acceptable range by further averaging the normal vector components from the two adjacent elements in curve smooth boundary. However, the success of those treatments needs further in depth research.

Comparing the present indirect algorithm with the direct ones [Frangi and Guigiani (2000); Karami and Derakhshan (1999); Gallego and Martinez-Castro (2006)], we find that both of them are based on the integral representations of the second

derivatives of field variables, therefore a full integration to the problem boundary is needed. Furthermore, the first derivative values at the source point are used for the regularization procedure in these two algorithms. However, the direct algorithms regularize the singular integrals before integration and the regularization procedure relates to the local variation of the field variable only, thus they seem to be more general than the present indirect one. The bootstrapping algorithm proposed by Schwab and Wendland (1999) and the limiting formulation proposed by Moore et al. (2007) are seminal contributions in this research, however they should be further developed for realistic problem solving. Furthermore, a number of existing algorithms are of the potential to be extended to the calculation of field variable second derivatives. Atluri (2005) has shown that the method of regularization of the BIE for the first derivative values [Okada et al. (1988, 1989, 1990); Okada and Atluri (1994)] can be easily extended to regularizing the BIEs for any order derivative of the primary variable. The multi-variable algorithm [Chen et al. (2005a); Schnack and Chen (2001)] could also be extended to combine together the boundary integral equations of the primary variable and its first and second derivatives. It would be significant to carefully compare the validities of the above diverse algorithms and to make clear the boundary a method is suitable for application.

6 Conclusions

A simple but effective algorithm is presented in this paper for the calculation of potential second derivatives at the boundary in 2D potential BEM. This algorithm is based on the regularized BIE formulation of potential second derivatives. The direct discretizations to the regularized formulations are implemented, where the original boundary values and the quadratic regularized function are interpolated completely in the same way to ensure the elimination of the singularities occurred in the potential second derivative BIEs. Numerical results show the validity of the present algorithm.

Acknowledgement: The support of the Natural Science Foundation of China (No. 10975130) is gratefully acknowledged. This research was partially done when the first author worked as a visiting professor at Shinshu University during August to December, 2007.

References

- Atluri, S. N. (2005): *Methods of Computer Modeling in Engineering & the Sciences*, Tech Science Press.
- Atluri, S. N.; Han, Z. D.; Shen, S. (2003): Meshless local Petrov-Galerkin (MLPG)

approaches for solving the weakly-singular traction & displacement boundary integral equations, *CMES: Computer Modeling in Engineering and Sciences*, vol. 4, no. 5, pp. 507-517.

Babuška, I.; Yu, D. (1987): Asymptotically exact *a*-posteriori error estimator for biquadratic elements, *Finite Elements in Analysis and Design*, vol. 3, pp. 341–54.

Bonnet, M. (1995): Regularized BIE formulations for first- and second-order shape sensitivity of elastic fields, *Computers and Structures*, vol. 56, no. 5, pp. 799–811.

Bonnet, M. (1997): Differentiability of strongly singular and hypersingular boundary integral formulations with respect to boundary perturbations, *Computational Mechanics*, vol. 19, pp. 240–246.

Bonnet, M.; Guiggiani, M. (1998): Tangential derivative of singular boundary integrals with respect to the position of collocation points, *International Journal of Numerical Method in Engineering*, vol. 41, pp. 1255–1275.

Chen, H. B. (2004): A regularized algorithm for the calculation of second derivative values in potential BEM (abstract), In: *Computational Mechanics, Proceedings of WCCM VI in conjunction with APCOM'04*, Tsinghua University Press & Springer-Verlag, pp. 36.

Chen, H. B.; Lu, P.; Huang, M. G.; Williams, F. W. (1998): An effective method for finding values on and near boundaries in the elastic BEM, *Computers and Structures*, vol. 69, no. 4, pp. 421–431.

Chen, H. B.; Lu, P.; Schnack, E. (2001): Effective algorithms for the calculation of values on and near boundaries in 2D elastic BEM, *Engineering Analysis with Boundary Elements*, vol. 25, pp. 851–876.

Chen, H. B.; Yu, D. H.; Schnack, E. (2003): A simple *a*-posteriori error estimation for adaptive BEM in elasticity, *Computational Mechanics*, vol. 30, pp. 343–354.

Chen, H. B.; Jin, J. F.; Zhang, P. Q.; Lu, P. (2005a): A Multi-variable Non-singular BEM in 2D Potential Problem, *Tsinghua Science and Technology*, vol. 10, no. 1, pp. 43–50.

Chen, H. B.; Guo, X. F.; Yu, D. H. (2005b): Regularized hyper-singular boundary integral equations for error estimation and adaptive mesh refinement, *Building Research Journal*, vol. 53, no. 1, pp. 33-44.

Chen, H. B.; Howson, W. P.; Lu, P.; Williams, F. W. (2009): An effective method for calculating values on and near boundaries in BEM for potential problems, In: *Advances and Application of Computational Mechanics*, Editor Youcheng WANG, Press of Hefei University of Technology, ISBN 978-7-5650-0098-0.

Frangi, A.; Guiggiani, M. (2000): A direct approach for boundary integral equa-

tions with high-order singularities, *International Journal of Numerical Method in Engineering*, vol. 49, pp. 871–898.

Gallego, R.; Martinez-Castro, A. E. (2006): Boundary integral equation for tangential derivative of flux in Laplace and Helmholtz equations, *International Journal of Numerical Method in Engineering*, vol. 66, pp. 334–363.

Gao, X. W. (2006): Numerical evaluation of two-dimensional singular boundary integrals—Theory and Fortran code, *Journal of Computational and Applied Mathematics*, vol. 188, pp. 44–64.

Guiggiani, M. (1996): Sensitivity analysis for boundary element error estimation and mesh refinement, *International Journal of Numerical Method in Engineering*, vol. 39, pp. 2907–2920.

Guiggiani, M.; Krishnasamy, G.; Rudolphi, T. J.; Rizzo, F. J. (1992): A general algorithm for the numerical solution of hypersingular boundary integral equations, *ASME Journal of Applied Mechanics*, vol. 59, pp. 604–614.

Han, Z. D.; Atluri, S. N. (2003): On simple formulations of weakly-singular traction & displacement BIE, and their solutions through Petrov-Galerkin approaches, *CMES: Computer Modeling in Engineering and Sciences*, vol. 4, no. 1, pp. 5–20.

Han, Z. D.; Atluri, S. N. (2007): A systematic approach for the development of weakly-singular BIEs, *CMES: Computer Modeling in Engineering & Sciences*, vol. 21, no. 1, pp. 41–52.

Han, Z. D.; Yao, Z. H.; Atluri, S. N. (2005): Weakly-singular traction and displacement boundary integral equations and their meshless local petrov-galerkin approaches, *Tsinghua Science and Technology*, vol. 10, no. 1, pp. 1–7.

Hou, J. W.; Sheen, J. (1993): Numerical methods for second-order shape sensitivity analysis with applications to heat conduction problems, *International Journal of Numerical Method in Engineering*, vol. 36, pp. 417–435.

Ilinca, F.; Pelletier, D. (2007): Computation of accurate nodal derivatives of finite element solutions: The finite node displacement method, *International Journal of Numerical Method in Engineering*, vol. 71, pp. 1181–1207.

Jin, J. F.; Chen, H. B. (2004): A new error indicator for 3D elastic BEM, *Journal of Yanshan University*, vol. 28, no. 1, pp. 70–73 (in Chinese).

Kane, J. H.; Mao, S.; Everstine, G. C. (1991): A boundary element formulation for acoustic shape sensitivity analysis, *The Journal of the Acoustical Society of America*, vol. 90, no. 1, pp. 561–573.

Karami, G.; Derakhshan, D. (1999): An efficient method to evaluate hypersingular and supersingular integrals in boundary integral equations analysis, *Engineering Analysis with Boundary Elements*, vol. 23, pp. 317–326.

Kita, E.; Kamiya, N. (2001): Error estimation and adaptive mesh refinement in boundary element method, an overview, *Engineering Analysis with Boundary Elements*, vol. 25, pp. 479–495.

Kita, E.; Kataoka, Y.; Kamiya, N. (1999): First- and second-order design sensitivity analysis scheme based on Trefftz method, *Trans. ASME: Journal of Mechanical Design*, vol. 121, no. 1, pp. 84-91.

Martinez-Castro, A. E.; Gallego, R. (2005): Tangential residual as error estimator in the boundary element method, *Computers and Structures*, vol. 83, pp. 685–699.

Matsumoto, T.; Tanaka, M.; Miyagawa, M.; Ishii, N. (1993): Optimum design of cooling lines in injection moulds by using boundary element design sensitivity analysis, *Finite Elements in Analysis and Design*, vol. 14, pp. 177-185.

Moore, M. N. J.; Gray, L. J.; Kaplan, T. (2007): Evaluation of supersingular integrals: second-order boundary derivatives, *International Journal of Numerical Method in Engineering*, vol. 69, pp. 1930–1947.

Moore, P. K. (2004): Interpolation error-based a posteriori error estimation for hp-refinement using first and second derivative jumps, *Appl. Numer. Math.*, vol. 48, pp. 63–82.

Okada, H.; Atluri, S. N. (1994): Recent developments in the field-boundary element method for finite/small strain elastoplasticity, *International Journal for Solids and Structures*, vol. 31, no. 12/13, pp. 1737-1775.

Okada, H.; Rajiyah, H.; Atluri, S. N. (1988): A novel displacement gradient boundary element methods for elastic stress analysis with high accuracy, *Journal of Applied Mechanics*, vol. 55, pp. 786-794.

Okada, H.; Rajiyah, H.; Atluri, S. N. (1989): Non-hyper-singular integral-representations for velocity (displacement) gradients in elastic/plastic solids, *Computational Mechanics*, vol. 4, no. 3, pp. 165-175.

Okada, H.; Rajiyah, H.; Atluri, S. N. (1990): A full tangent stiffness field-boundary element formulation for geometric and material nonlinear problems of solid mechanics, *International Journal of Numerical Method in Engineering*, vol. 29, pp. 15-35.

Qian, Z. Y.; Han, Z. D.; Atluri, S. N. (2004a): Directly derived non-hyper-singular boundary integral equations for acoustic problems, and their solution through Petrov-Galerkin schemes, *CMES: Computer Modeling in Engineering and Sciences*, vol. 5, no. 6, pp. 541-562.

Qian, Z. Y.; Han, Z. D.; Ufimtsev, P.; Atluri, S. N. (2004b): Non-hyper-singular boundary integral equations for acoustic problems, implemented by the collocation-based boundary element method, *CMES: Computer Modeling in Engineering &*

Sciences, vol. 6, no. 2, pp. 133-144.

Schnack, E.; Chen, H. B. (2001): A multi-variable non-singular BEM in 2D elasticity, *European Journal of Mechanics, A/solids*, vol. 20, pp. 645-659.

Schwab, C.; Wendland, W. L. (1999): On the extraction technique in boundary integral equations. *Mathematics of Computation*, vol. 68, no. 225, pp. 91-122.

Sladek, V.; Sladek, J. (eds) (1998): *Singular Integrals in Boundary Element Methods*, Computational Mechanics Publications, Southampton.

Sladek, V.; Sladek, J.; Tanaka, M. (2003): Regularization of hypersingular and nearly singular integrals in the potential theory and elasticity, *International Journal of Numerical Method in Engineering*, vol. 36, no. 10, pp. 1603–1628.

Telles, J. C. F.; Prado, A. A. (1993): Hyper-singular formulation for 2D potential problems. In: *Advanced Formulations in Boundary Element Methods*, Computational Mechanics Publications.

Yazdani, A. A.; Gakwaya, A.; Dhatt, G. (1997): A posteriori error estimator based on the second derivative of the displacement field for two-dimensional elastic problems, *Computers and Structures*, vol. 62, no. 2, pp. 317–338.

Yu, D. (1991a): Asymptotically exact a-posteriori error estimator for elements of bi-even degree, *Math. Numer. Sinica*, vol. 19, pp. 89–101.

Yu, D. (1991b): Asymptotically exact a-posteriori error estimator for elements of bi-odd degree, *Math. Numer. Sinica*, vol. 19, pp. 307–314.

Zhang, Q.; Mukherjee, S. (1991): Second-order design sensitivity analysis for linear elastic problems by the derivative boundary element method, *Computer Methods in Applied Mechanics and Engineering*, vol. 86, no. 3, pp. 321–335.

Zienkiewicz, O. C. (2006): The background of error estimation and adaptivity in finite element computations, *Computer Methods in Applied Mechanics and Engineering*, vol. 195, pp. 207–213.